

# Supporting Information

## Efficient Synthesis of Tailored Magnetic Carbon Nanotube via a Noncovalent Chemical Route

Xianglong Li,<sup>\*a</sup> Joe D. Thompson,<sup>b</sup> Yingying Zhang,<sup>a</sup> Christina I. Brady,<sup>c</sup> Guifu Zou,<sup>a</sup> Nathan  
H. Mack,<sup>c</sup> Darrick Williams,<sup>a</sup> Juan G. Duque,<sup>c</sup> Quanxi Jia,<sup>a</sup> and Stephen K. Doorn<sup>\*a</sup>

<sup>a</sup>Center for Integrated Nanotechnologies, Materials Physics and Applications Division, <sup>b</sup>  
Condensed Matter and Magnet Science, Materials Physics and Applications Division, and <sup>c</sup>  
Physical Chemistry and Applied Spectroscopy, Chemistry Division, Los Alamos National  
Laboratory, Los Alamos, New Mexico, 87545 USA

E-mail: [xianglongli@lanl.gov](mailto:xianglongli@lanl.gov); [skdoorn@lanl.gov](mailto:skdoorn@lanl.gov)

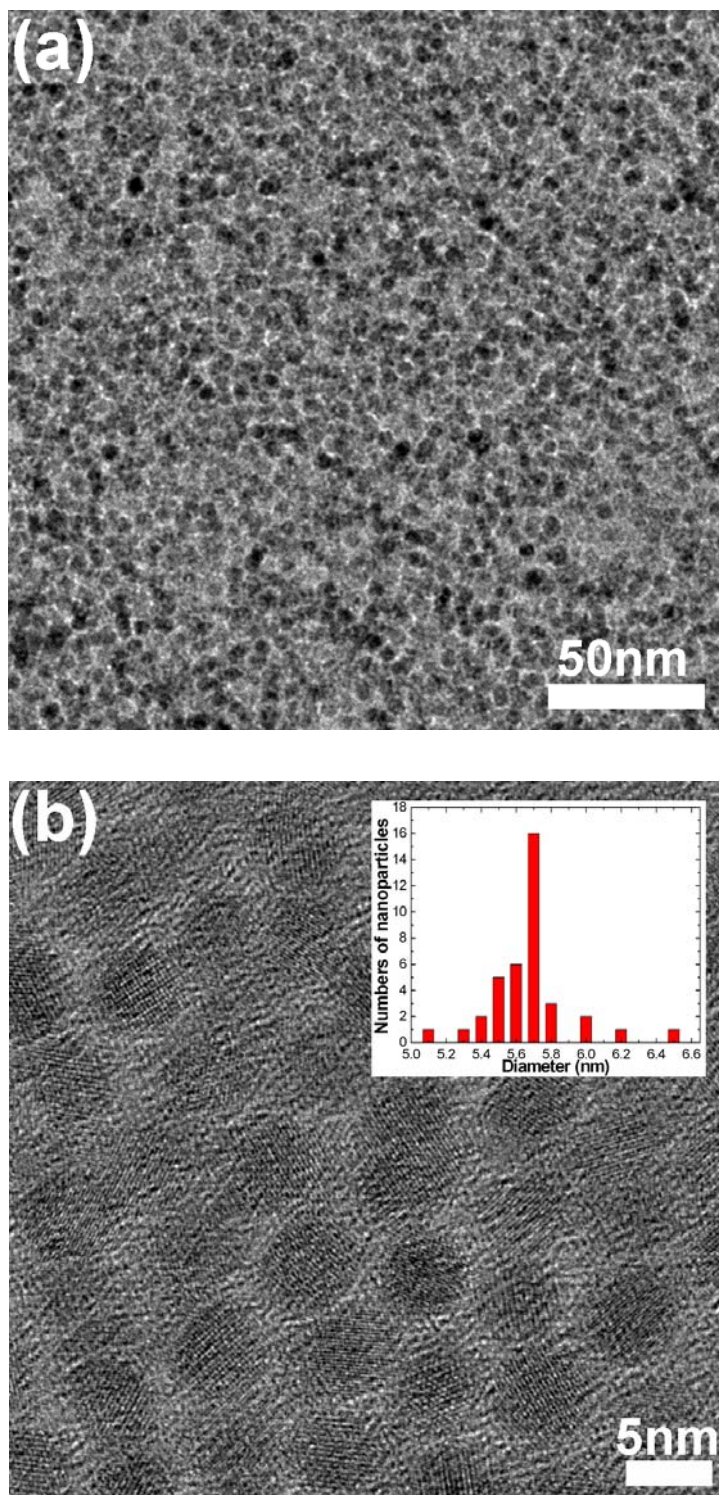


**Figure S1.** (a) A typical TEM image of the as-synthesized MNPs. (b) High resolution TEM image of the MNPs with size distribution histogram.

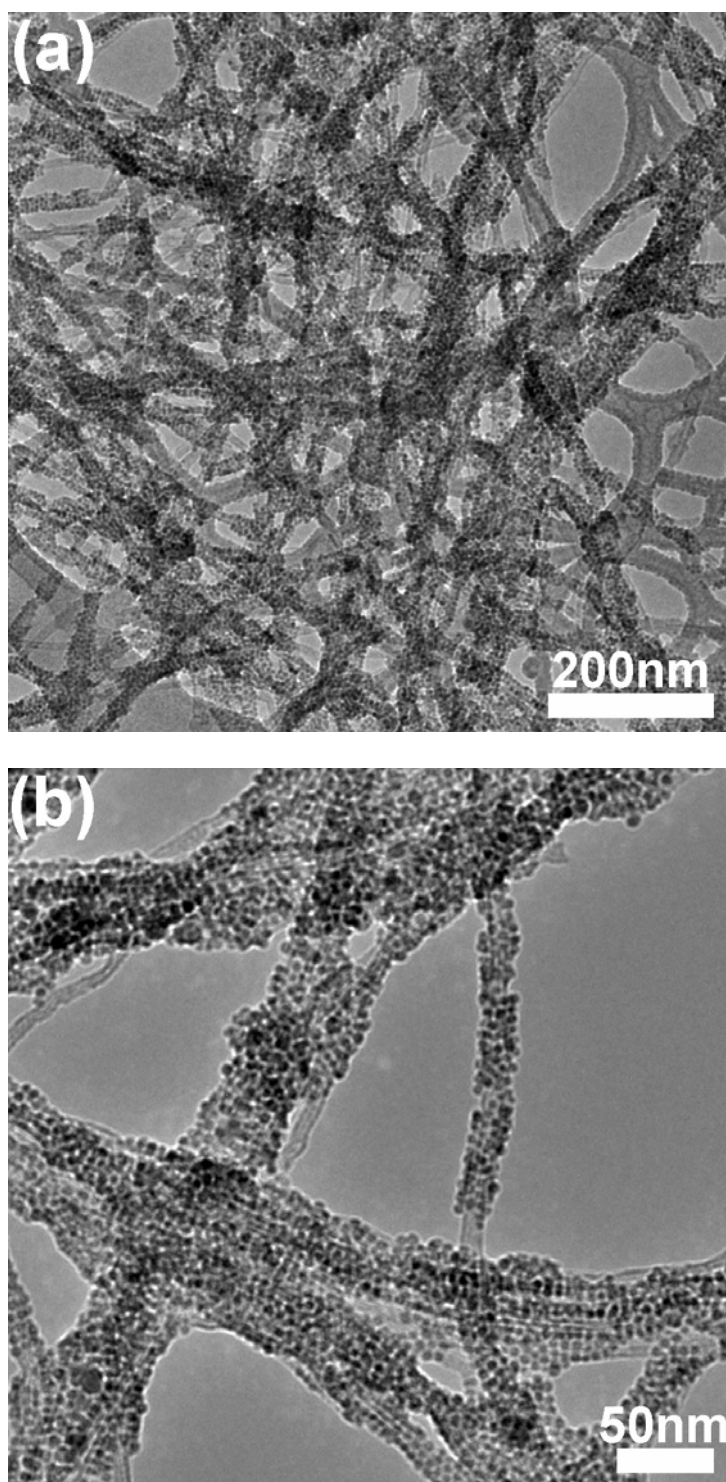


**Figure S2.** TEM images of the MNP-MWNT hybrids.

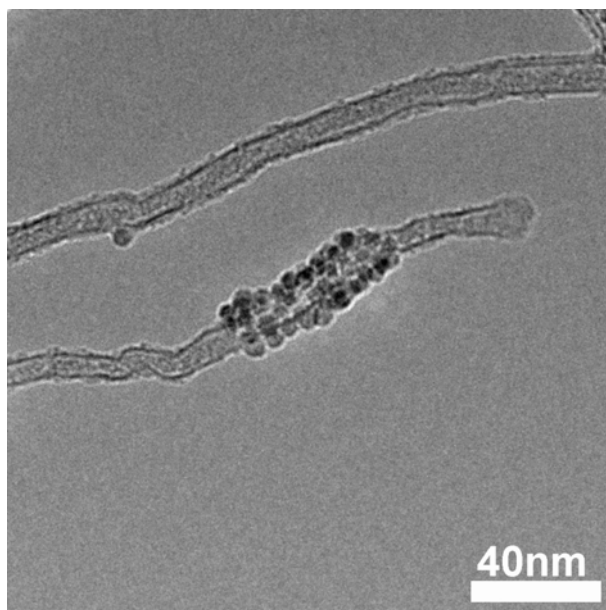


**Figure S3.** A typical TEM image of MNP-MWNT hybrids (with a 2 wt % nanoparticle content).

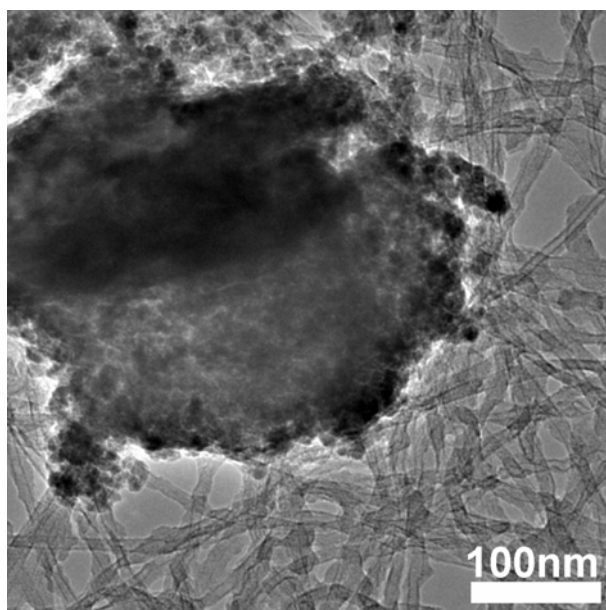


**Figure S4.** A typical TEM image of a simple physical mixture of the MNPs and the nanotubes obtained by employing the pristine MWNTs as a support.

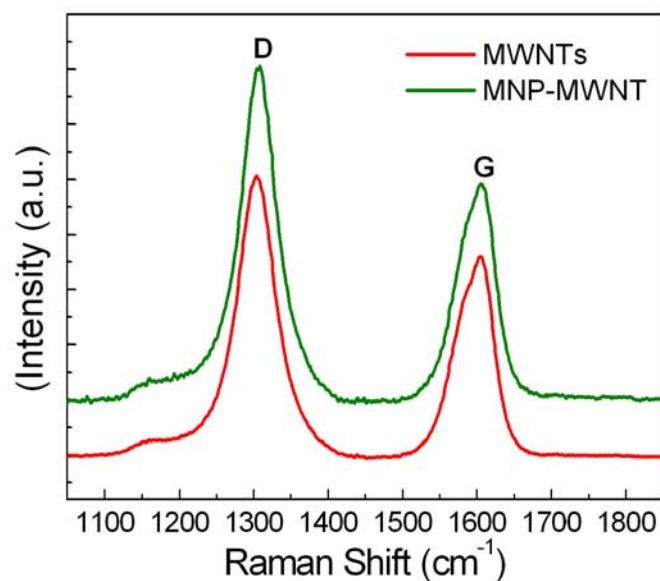


**Figure S5.** Raman spectra of the MWNTs and the MNP-MWNT hybrids. The spectra were vertically offset for clarity. Both of the spectra show a G band at ca. 1606 cm<sup>-1</sup>, and a disorder-induced D band at ca. 1305 cm<sup>-1</sup> of the nanotubes. The relative intensity ratio of the D band to the G band is nearly identical for the as-produced MWNTs (1.41) and the hybrids (1.43).

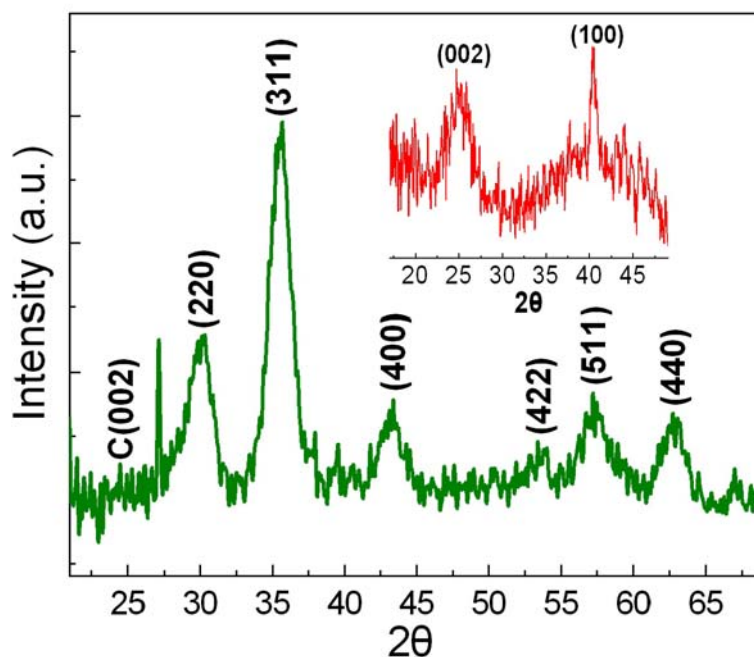


**Figure S6.** Typical XRD pattern of the MNP-MWNT hybrids. Inset: XRD pattern of the MWNT array. For the as-grown MWNT arrays (inset), the diffraction pattern shows two peaks at ca. 25.2 and 40.4°, corresponding to the (002) and (100) planes of the graphite structure, respectively. In the pattern for the hybrids all well-resolved reflection peaks at 30.1, 35.5, 43.1, 53.7, 57.4, and 62.8° can be respectively indexed to the (220), (311), (400), (422), (511), and (440) planes of the face-centered cubic structure of the assembled maghemite nanoparticles (JCPDS card no. 39-1346). It is well-known that the broadness of the peak increases with the decrease in the particle size.<sup>1,2</sup> Therefore, the obviously broadened peaks of the here-assembled MNPs suggests their nanocrystallite nature. The particle size estimated by Scherrer's formula using the (311) peak was about 5 nm, which is close to the above TEM results. Furthermore, it is difficult to distinguish the (002) peak of the nanotubes in the pattern for the hybrids, which is probably related to the fact that a weaker (002) peak is obtained even if in the case of the as-grown nanotubes.

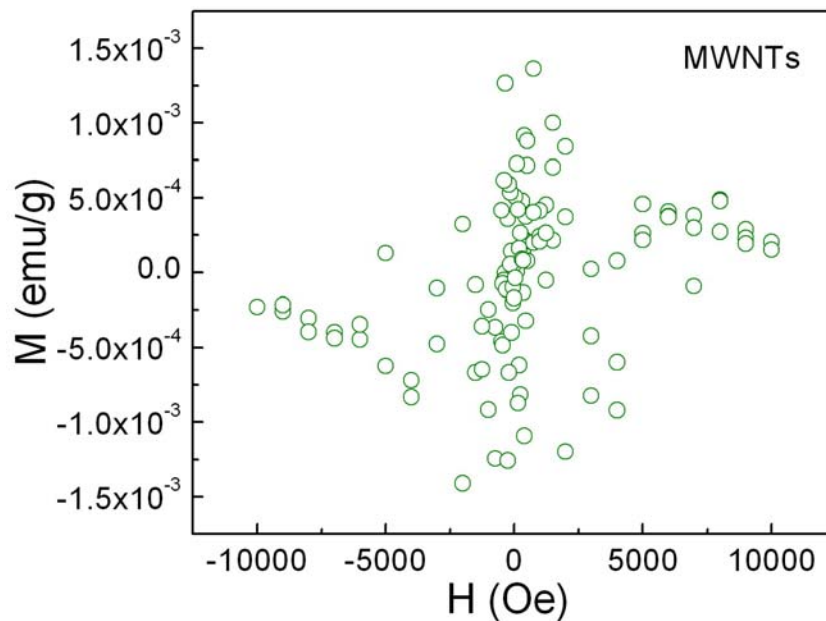


**Figure S7.** Hysteresis curves measured at 300 K for the MWNTs showing the pristine nanotubes are nonmagnetic.

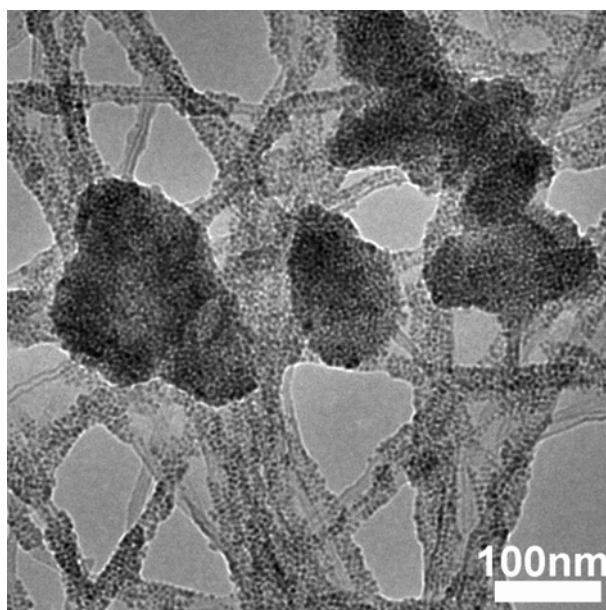


**Figure S8.** A typical TEM image of the  $\gamma$ -Fe<sub>2</sub>O<sub>3</sub> nanoparticle-MWNT composite (with a 15 wt % nanoparticle content) synthesized *via* the here-presented assembly route, showing that the introduction of too much MNPs results in formation of undesirable nanoparticle agglomerates.

**References:**

- 1 Bourlinos, A.; Simopoulos, A.; Petridis, D.; Okumura, H.; Hadjipanayis, G. *Adv. Mater.* **2001**, *13*, 289-291.
- 2 Santra, S.; Tapeç, R.; Theodoropoulou, N.; Dobson, J.; Hebard, A.; Tan, W. *Langmuir* **2001**, *17*, 2900-2906.